

Suppression of Superconductivity in $\text{Lu}_x\text{Zr}_{1-x}\text{B}_{12}$: Evidence of Static Magnetic Moments Induced by Non-Magnetic Impurities

N.E.Sluchanko^{1,*}, A.N.Azarevich¹, M.A.Anisimov¹, A.V.Bogach¹, S.Yu.Gavrilkin²,

V.V.Glushkov^{1,3}, S.V.Demishev^{1,3}, A.L.Khoroshilov³, A.V.Dukhnenko⁴,

K.V.Mitsen², N.Yu.Shitsevalova⁴, V.B.Filippov⁴, V.V.Voronov¹, and K.Flachbart⁵

¹ – *A.M.Prokhorov General Physics Institute of RAS, 38 Vavilov Street, 119991 Moscow Russia*

² – *P.N.Lebedev Physical Institute of RAS, Moscow, 119991 Russia*

³ – *Moscow Institute of Physics and Technology, 141700 Dolgoprudnyi, Russia*

⁴ – *Institute for Problems of Materials Science of National Academy of Sciences of Ukraine, 3 Krzhizhanovskogo Street, 03680 Kiev, Ukraine and*

⁵ – *Institute of Experimental Physics of SAS, 47 Watsonova Street, SK-04001 Kosice, Slovak Republic*

(Dated: January 25, 2021)

Based on low temperature resistivity, heat capacity and magnetization investigations we show that the unusually strong suppression of superconductivity in $\text{Lu}_x\text{Zr}_{1-x}\text{B}_{12}$ BSC-type superconductors in the range $x < 0.08$ is caused by the emergence of static spin polarization in the vicinity of non-magnetic lutetium impurities. The analysis of received results points to a formation of static magnetic moments with $\mu_{eff} \approx 3\mu_B$ per Lu-ion. The size of these spin polarized nanodomains was estimated to be about 5 Å.

PACS numbers: 74.70.Ad, 74.62.-c

1. The discovery of superconductivity at $T_C \approx 39$ K in MgB_2 [1] stimulated a significant interest into the studies of a wide class of the alkaline-earth, rare-earth and transition-metal borides. Among them, in the family of higher borides RB_{12} , zirconium dodecaboride (ZrB_{12}) is a BCS superconductor with the highest $T_C \approx 6$ K [2, 3]. An intriguing detail established for ZrB_{12} is the formation of Cooper pairs through quasi-local vibrations involving Zr^{4+} ions located within truncated B_{24} octahedrons in the UB_{12} -type *fcc* crystal structure [2]-[5]. In studies of the Einstein phonon mediated superconductivity in ZrB_{12} authors of [2]-[9] argue that *s*-wave pairing is characteristic for this compound, and that in this case the Ginzburg-Landau parameter κ is located in the nearest vicinity of the threshold value $\kappa_C = 2^{-1/2}$. Moreover, a crossover from type-I to type-II/1 superconductivity with temperature lowering was deduced in [3] from heat capacity and magnetization measurements. In contrast, in [10] the superconductivity in ZrB_{12} was interpreted in terms of *d*-wave pairing and a two-gap type-II regime was identified with parameters $\kappa_p = 3.8$ and $\kappa_d = 5.8$. Additionally, a large size pseudo-gap ($\Delta \sim 7.3$ meV) has been detected employing high resolution photoemission spectroscopy in ZrB_{12} above T_C , and proximity to the quantum fluctuation regime was predicted from *ab initio* band structure calculations [11]. Thus, also similarities with cuprate high temperature superconductors (HTSC) may be supposed to revive the interest into studies of this low temperature superconductor.

In case of non-magnetic impurity substitutions and their impact on superconducting properties one can choose between various scenarios, because for these

defects the pair-breaking mechanism in various models differs. According to Anderson's theorem [12, 13] and its extension to non-*s*-wave superconductivity (see e.g. [14, 15]) already a small amount of non-magnetic impurities can dramatically suppress superconductivity by pair-breaking in the case of anisotropic gap in a *d*-wave superconductor. Moreover, experiments on cuprates reveal [15] that a spinless impurity (Zn, Li etc.) introduced into a HTSC host produces in its vicinity a large and spatially extended alternating magnetic polarization. On the basis of NMR and μSR spectra it has been demonstrated that this impurity-induced magnetization on the nearest neighbor Cu atoms in cuprates is associated with a dynamic moment [15].

In the case of RB_{12} the replacement of non-magnetic ions of Zr by Lu produces an about 15 times' reduction of superconducting transition temperature ($T_C \approx 0.4$ K for LuB_{12} [4, 9, 16]), and the origin of this large T_C suppression is not cleared up to now for these two compounds with similar conduction bands and crystalline structures. Indeed, inelastic neutron scattering studies of the phonon spectra in LuB_{12} and ZrB_{12} [5] have detected noticeable, but not dramatic changes in the position of almost dispersion-less quasi-local mode (15 meV and 17.5 meV, correspondingly), which was proposed to be responsible for Cooper pairing. Only a moderate difference in the electronic density of states of these two compounds is caused by filling of a wide enough conduction band ($\sim 1.6 \div 2$ eV) when Lu^{3+} – ion is changed to Zr^{4+} in the RB_{12} unit cell, resulting to an elevation by about 0.3-0.4 eV of the Fermi level E_F for ZrB_{12} in comparison to LuB_{12} [11, 17].

Here we probed the evolution of superconducting transition temperature T_C and the normal state parameters for substitutional solid solutions $\text{Lu}_x\text{Zr}_{1-x}\text{B}_{12}$ employing resistivity, heat capacity

*Electronic address: nes@lt.gpi.ru

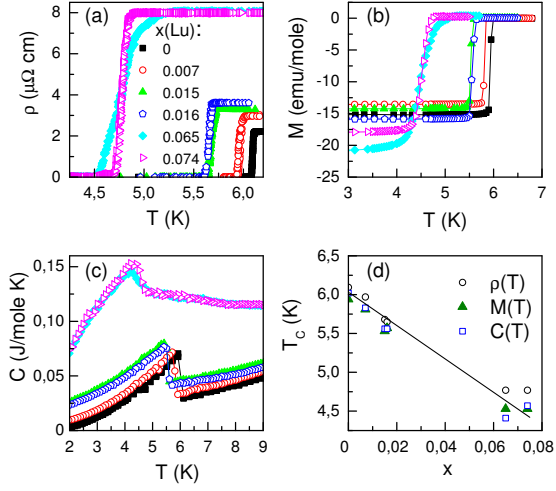


Fig. 1: (Colour on-line) Temperature dependences of (a) resistivity, (b) magnetization at $H=5$ Oe and (c) specific heat in vicinity of T_C , and (d) the suppression of superconductivity $T_C(x)$ in $\text{Lu}_x\text{Zr}_{1-x}\text{B}_{12}$.

and magnetization measurements. It will be shown that the non-magnetic Lu impurity substitution (having a $4f^{14}$ configuration) produces a strong static spin polarization in the RB_{12} matrix in the vicinity of lutetium ions. Simultaneously with the emergence of static magnetic moments with a value of about $3\mu_B$ per Lu ion the received experimental results exhibit a strong suppression of superconductivity in $\text{Lu}_x\text{Zr}_{1-x}\text{B}_{12}$.

2. Studies of resistivity, transverse magnetoresistance, heat capacity and magnetization of high-quality single crystals of $\text{Lu}_x\text{Zr}_{1-x}\text{B}_{12}$ solid solutions with $x < 0.08$ were carried out at temperatures in the range 1.8-300 K, in magnetic fields of up to 90 kOe ($\mathbf{H} \parallel \langle 001 \rangle$). A standard *dc* four probe technique was applied for resistivity investigation with the orientation of measuring current $\mathbf{I} \parallel \langle 110 \rangle$. Magnetization and heat capacity were measured using a PPMS-9 (Quantum Design). The single crystals of $\text{Lu}_x\text{Zr}_{1-x}\text{B}_{12}$ were grown by vertical crucible-free inductive floating zone melting in an inert gas atmosphere. To verify the samples' quality and the Lu content X-rays Laue back-pattern (see Fig.S1 in the [Supplementary Information](#)) and microanalysis techniques were applied.

3. Temperature dependences of resistivity (fig.1a), magnetization (fig.1b) and heat capacity (fig.1c) show superconducting phase transitions with T_C in the range 4.5-6 K for $\text{Lu}_x\text{Zr}_{1-x}\text{B}_{12}$ ($x < 0.08$) solid solutions. The resistivity $\rho(T)$ drop to zero below T_C is accompanied both with the appearance of Meissner state diamagnetic response on $M(T)$ curves and the stepwise changes in the specific heat $C(T)$ (see fig.1 and figs.2a-b, $H=0$ curves). With the increase of lutetium content both the residual resistivity and the normal state specific heat rise dramatically (by a factor of 4, see fig.1a and figs.2a

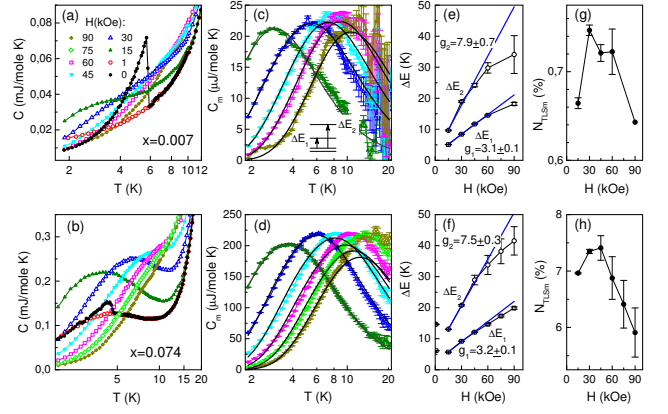


Fig. 2: (Colour on-line) Temperature dependences of specific heat for $\text{Lu}_x\text{Zr}_{1-x}\text{B}_{12}$ with (a) $x=0.007$ and (b) $x=0.074$ in magnetic field up to 90 kOe. Panels (c) and (d) demonstrate the separated magnetic component C_m of heat capacity for Lu content $x=0.007$ and $x=0.074$, correspondingly. The fitting of $C_m(T, H_0)$ by three-level Schottky relation (see scheme on panel (c)) is shown by solid lines. The splitting energies $\Delta E_1(H)$, $\Delta E_2(H)$ and concentrations $N_{TLSm}(H)$ are shown for $\text{Lu}_x\text{Zr}_{1-x}\text{B}_{12}$ with $x=0.007$ and 0.074 on panels (e),(f) and (g),(h), correspondingly.

and 2b), and the later one demonstrates a combination of superconducting step-like and Schottky-type anomaly (see e.g. fig.2b, $H=0$ curve for $x=0.074$). It is worth to note that the Schottky anomaly for $\text{Lu}_{0.074}\text{Zr}_{0.0926}\text{B}_{12}$ (fig.2b, $H=0$) is very similar to that one observed previously for LuB_{12} [9, 18, 19], and it may be interpreted in terms of formation of two-level systems (TLS) in the disordered RB_{12} matrix of this cage-glass compound. The $T_C(x)$ dependence for $\text{Lu}_x\text{Zr}_{1-x}\text{B}_{12}$ solid solutions is summarized in fig.1d. It should be stressed that the suppression of superconductivity by Lu substitution is unusually strong (~ 0.21 K/at.% Lu), when supposing the doping of an *s*-wave superconductor by non-magnetic impurities.

In external magnetic field the amplitude of the low temperature Schottky anomaly increases essentially and $C(T)$ maximum moves to higher temperatures (for example, figs.2a, 2b show the data for $x=0.007$ and 0.074, correspondingly). Evidently, the Zeeman component is a magnetic contribution to heat capacity and it may be separated from vibrational and electron heat capacity terms following the approach developed in [18, 19]. The resulting $C_m(T, H_0)$ dependences are presented in figs.2c, 2d for these two Lu contents together with their approximation (see solid lines in figs.2c, 2d) based on a three-level Schottky relation (see eq.(S1) in [supplementary materials](#)) (the scheme presented in insert to fig.2c). Both splitting energies $\Delta E_1(H)$, $\Delta E_2(H)$ and the concentration of magnetic Schottky sites $N_{TLSm}(H)$ as deduced from the approximation are shown on figs.2e,

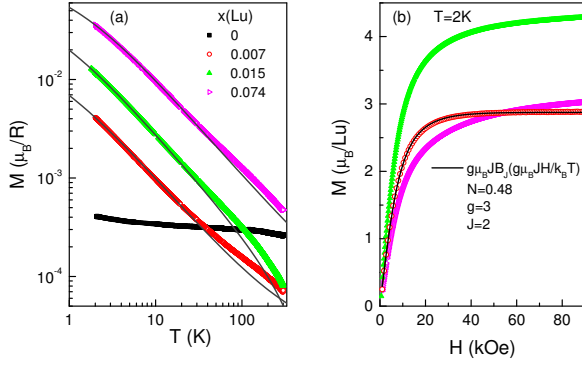


Fig. 3: (Colour on-line) Dependences of magnetization vs. temperature at $H=2$ kOe (a) and vs. magnetic field at $T=2$ K (b) for $\text{Lu}_x\text{Zr}_{1-x}\text{B}_{12}$. Approximations by Curie-Weiss relation (1) (panel (a)) and by Brillouin dependence (2) (panel (b)) are shown by solid lines.

$2g$ and figs.2f, 2h, correspondingly. The slope of straight lines on figs.2e and 2f (in the range $H < 40$ kOe) allows to determine the g -factors from relation $\Delta E_i = \mu_B g_i H / k_B$ and obtain the values $g_1 \sim 3.2$ and $g_2 \sim 7.8$ for both studied crystals. Moreover, the concentration of TLsm is found to be within experimental accuracy equal to x values in $\text{Lu}_x\text{Zr}_{1-x}\text{B}_{12}$. From these results it may be concluded that magnetic sites are created by Lu substitution.

The magnetic response in the normal state of $\text{Lu}_x\text{Zr}_{1-x}\text{B}_{12}$ superconductors was investigated by magnetization $M(H, T)$ studies. Figs.3a and 3b demonstrate the temperature dependences $M(H_0, T)$ recorded at $H_0=2$ kOe and the magnetization vs. magnetic field curves $M(H, T_0)$ measured at $T_0=2$ K, correspondingly. It can be seen from fig.3a, that a small ($\sim 4 \times 10^{-4} \mu_B/\text{Zr}$) and about temperature independent Pauli-like paramagnetic response, which is typical for ZrB_{12} , changes into a Curie-Weiss-type magnetic signal originating from localized magnetic moments induced by the Lu substitution. Fitting the temperature dependences by Curie-Weiss relation

$$M = \chi_0 H + \mu_{eff}^2 H / (k_B(T - \Theta)) \quad (1)$$

where χ_0 - temperature independent susceptibility, k_B - Boltzman constant and Θ - Curie-Weiss temperature (see solid lines in fig.3a) allows to determine the Curie constant and subsequently to estimate the effective magnetic moment $\mu_{eff} \sim 3.3-3.8 \mu_B$ per Lu ion (see also Tab.S1 in the Supplementary materials). These values correlate very well with the saturated moments $\mu_S \sim 3-4 \mu_B$ per Lu ion obtained from the analysis of magnetization vs. magnetic field dependences (fig.3b).

Moreover, in the regime of isolated magnetic impurity for $x=0.007$ the magnetization may be described with a good accuracy by the Brillouin-type dependence

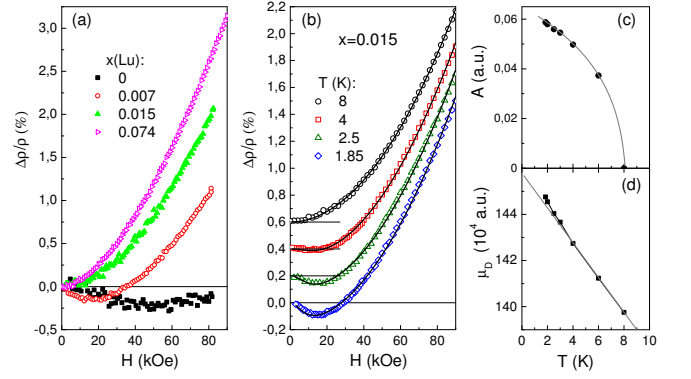


Fig. 4: (Colour on-line) Magnetic field dependences of normal state magnetoresistance $\Delta\rho/\rho(H, T_0)$ (a) for $\text{Lu}_x\text{Zr}_{1-x}\text{B}_{12}$ with various Lu content at $T_0=4.5$ K, and (b) for $x=0.015$ at temperatures in the range 1.85-8 K. Approximations in the framework of (eq.4) are shown by solid lines in panel (b); curves are shifted by 0.2% for convenience. Panels (c) and (d) demonstrate temperature dependences of A and μ_D parameters in (eq.4).

$$M = N_m g \mu_B J B_J(g \mu_B J H / k_B T) \quad (2)$$

(where N_m —concentration of magnetic sites, B_J —Brillouin function, μ_B —Bohr magneton and J —angular momentum) with $N_m \approx 0.48x$, $g \approx 3$ and $J \approx 2$. As a result, it encourages us to suggest as a simplest scenario that impurity ions of Lu are combined into dimers with a magnetic moment $\mu_S = gJ = 6 \mu_B$ and with a size equal to about $d(\text{Lu-Lu}) \sim 5.3 \text{ \AA}$ — the distance between heavy ions in the RB_{12} matrix, which can be considered as a formation of spin-polarized nanodomains in $\text{Lu}_x\text{Zr}_{1-x}\text{B}_{12}$.

Magnetoresistance $\Delta\rho/\rho$ experiments were also performed to characterize the magnetic moments in these compounds with metallic conduction. According to Yosida calculations carried out within the framework of s - d exchange model, an appearance of negative magnetoresistance (nMR) is expected in the regime of charge carrier scattering on localized magnetic moments [20]. Both field and temperature dependences of nMR are controlled by local magnetization M_{loc} through the relation

$$-\Delta\rho/\rho \sim M_{loc}^2. \quad (3)$$

The nMR effect may be considered as an independent argument in favor of local moments' formation in a metallic matrix. Fig.4 shows the results of magnetoresistance measurements on $\text{Lu}_x\text{Zr}_{1-x}\text{B}_{12}$. In the normal state of ZrB_{12} the main contribution to $\Delta\rho/\rho(H, T_0)$ is positive and it can be described with a

good accuracy by the well-known relation $\Delta\rho/\rho\sim\mu_D^2H^2$, where μ_D is the carriers' drift mobility. Both the substitutional disorder and the cage-glass effect in $\text{Lu}_x\text{Zr}_{1-x}\text{B}_{12}$ decrease dramatically both the mobility and amplitude of the positive component when Lu concentration increases (fig.4a). For $x\geq 0.015$ the appearance of nMR contribution to $\Delta\rho/\rho$ becomes evident, and for $x\sim 0.07$ the negative term in applied magnetic fields (fig.4a) prevails. Fig.4b presents a set of magnetic field dependences $\Delta\rho/\rho(H, T_0)$ obtained for $x=0.015$ at temperatures between 1.8 K and 8 K. In the range between 8 K and 4 K a crossover from positive magnetoresistance to a combination of positive and negative components is observed, and similar to the approach developed in [21], these data may be approximated very well by relation

$$\Delta\rho/\rho = -(Ag\mu_B JB_J(g\mu_B JH/k_B T))^2 + \mu_D^2 H^2. \quad (4)$$

Fitting data by relation (4) (see solid lines in fig.4b) allows to estimate the g-factor $g\approx 3.5$ and the angular momentum $J=2$. The obtained values are very close to those deduced above from the analysis of magnetization results by relation (2). Additionally, we have evaluated the behavior of coefficients $A(T)$ and $\mu_D(T)$ in (4) (see figs.4c and 4d, correspondingly). As can be seen from fig.4c, the scattering of charge carriers on localized moments in vicinity of impurity sites appears below 8 K and increases drastically with temperature lowering. On the contrary, the $\mu_D(T)$ dependence demonstrates only a moderate elevation with temperature decrease (fig.4d). Thus, these positive and negative components

of magnetoresistance become comparable at helium temperatures and in magnetic fields below 40 kOe.

When discussing the possible scenario of the formation of spin-polarized nanodomains in this case, it is worth to note the mechanism of spin-polaron formation proposed for the rare earth higher borides with a cage-glass structure. It was suggested in [22] that fast quantum oscillations of heavy rare earth ions in a double-well potential lead to spin polarization of $5d$ -conduction band states, and this effect appears to be very sensitive to external magnetic field. Turning to the analogy with non-magnetic impurity-induced *dynamic* moments in HTSC cuprates, it should be stressed here that the localized moments found in present study of $\text{Lu}_x\text{Zr}_{1-x}\text{B}_{12}$ are *static* and that a strong enhancement of spin polarization (exhibiting a saturation above 40 kOe) is induced by external magnetic field.

To summarize, we have found a formation of static magnetic moments with $\mu_{eff}\approx 3\mu_B$ per Lu-ion in the vicinity of non-magnetic lutetium impurities in the Zr-rich matrix of $\text{Lu}_x\text{Zr}_{1-x}\text{B}_{12}$ dodecaborides at low temperatures. According to our opinion, the strong suppression of superconductivity in $\text{Lu}_x\text{Zr}_{1-x}\text{B}_{12}$ compounds should be attributed to pair-breaking arising in the vicinity of these nanosize magnetic domains.

We would like to thank A.V.Kuznetsov, G.E.Grechnev and S.Gabani for helpful discussions. The study was supported by RFBR project No. 15-02-02553a, Young Scientists Grant of the RF President No. MK-6427.2014.2. The measurements were carried out in Shared Facility Centre of P.N.Lebedev Physical Institute of RAS.

-
- [1] J.Nagamatsu, N.Nakagawa, T.Muranaka et al., *Nature (London)* **410**, 63 (2001).
 [2] R.Lortz, Y.Wang, S.Abe et al., *Phys. Rev. B* **72**, 024547 (2005).
 [3] Y.Wang, R.Lortz, Yu.B.Paderno et al., *Phys. Rev. B* **72**, 024548 (2005).
 [4] J.Teyssier, R.Lortz, A. Petrovic et al., *Phys. Rev. B* **78**, 134504 (2008).
 [5] A.V.Rybina, K.S.Nemkovski, P.A.Alekseev et al., *Phys. Rev. B* **82**, 024302 (2010).
 [6] M.I.Tsindlekht, G.I.Leviev, I. Asulin et al., *Phys. Rev. B* **69**, 212508 (2004).
 [7] G.I.Leviev, V.M.Genkin, M.I.Tsindlekht et al., *Phys. Rev. B* **71**, 064506 (2005).
 [8] D.Daghero, R.S.Gonnelli, G.A.Ummarino et al., *Supercond. Sci. Technol.* **17**, S250 (2004).
 [9] N.Sluchanko, S.Gavrilkin, K.Mitsen et al., *J. Supercond. Nov. Magn.* **26**, 1663 (2013).
 [10] V.A.Gasparov, N.S.Sidorov, and I.I.Zver'kova, *Phys. Rev. B* **73**, 094510 (2006).
 [11] S.Thakur, D.Biswas, N.Sahadev, et al., *Sci. Rep.* **03342** (2013).
 [12] P.W.Anderson, *Phys. Rev. Lett.* **3**, 325 (1959).
 [13] A.A.Abrikosov, L.P.Gor'kov, *Zh. Exp. Theor. Phys.* **39**, 1781 (1960) [*Sov. Phys. JETP* **12**, 1243 (1961)].
 [14] A.V.Balatsky, I.Vekhter, J.X.Zhu, *Rev. Mod. Phys.* **78**, 373 (2006).
 [15] H.Alloul, J.Bobroff, M.Gabay, P.J.Hirschfeld, *Rev. Mod. Phys.* **81**, 45 (2009).
 [16] K.Flachbart, S.Gabani, K.Gloos et al., *J. Low Temp. Phys.* **140**, 339 (2005).
 [17] B.Jager, S.Paluch, O.J.Zogal et al., *J. Phys. Condens. Matter* **18**, 2525 (2006).
 [18] N.E.Sluchanko, A.N.Azarevich, A.V.Bogach et al., *JETP* **113**, 468 (2011).
 [19] N.E.Sluchanko, A.N.Azarevich, S.Yu.Gavrilkin et al., *JETP Lett.* **98**, 578 (2013).
 [20] K.Yosida, *Phys. Rev.* **107**, 396 (1957).
 [21] N.E.Sluchanko, A.L.Khoroshilov, M.A.Anisimov et al., *Phys. Rev. B* **91**, 235104 (2015).
 [22] N.E.Sluchanko, *Low Temp. Phys./Fizika Nizkikh Temperatur* **41**, 699 (2015).

SUPPLEMENTARY INFORMATION

1)

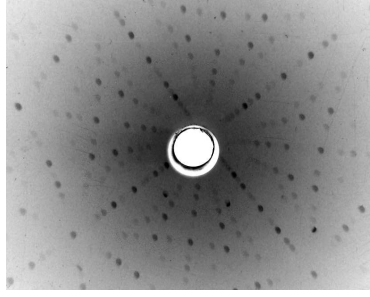


Fig. S1: X-ray Laue pattern from the lateral cross section of a raw single crystal $\text{Lu}_{0.074}\text{Zr}_{0.926}\text{B}_{12}$ grown with $[100]$ oriented seed. The growth direction deviation from $[100]$ is about 3 degree.

2) three-level Schottky relation:

$$C_m = N \frac{R}{\beta^2} \frac{2\Delta E_1^2 e^{-\beta\Delta E_1} + 2\Delta E_2^2 e^{-\beta\Delta E_2} + (\Delta E_1 - \Delta E_2)^2 e^{-\beta(\Delta E_1 + \Delta E_2)}}{(2 + e^{-\beta\Delta E_1} + e^{-\beta\Delta E_2})^2}, \beta = 1/k_B T \quad (\text{S1})$$

3)

Tab.S1: The parameters of heat capacity and magnetization analysis performed for $\text{Lu}_x\text{Zr}_{1-x}\text{B}_{12}$ on figs.2 and 3.

x	C			M		
	g_1	g_2	$N_{\text{TLSm}} (\%)$	$\mu_{\text{eff}} (\mu_B)$	$\mu_{\text{sat}} (\mu_B)$	$\chi_0 (\mu_B/\text{kOe})$
0.007	3.1 ± 0.1	7.9 ± 0.7	0.7 ± 0.04	3.3	2.88	$2.32 \cdot 10^{-5}$
0.015	3.3 ± 0.3	7.8 ± 0.2	2.1 ± 0.1	3.8	4.3	$-4.59 \cdot 10^{-5}$
0.016	3.0 ± 0.1	7.6 ± 0.7	1.8 ± 0.2			
0.065	3.5 ± 0.2	6.8 ± 0.1	7.2 ± 0.3			
0.074	3.2 ± 0.1	7.5 ± 0.3	6.8 ± 0.6	3.3	3.0	$3.27 \cdot 10^{-5}$